Phase transition of KDP observed by Resonant X-ray Diffraction at forbidden reflections

G. Beutier, S. P. Collins, E. N. Ovchinnikova, G. Nisbet, V. E. Dmitrienko

Phase transition of KDP observed by Resonant X-ray Diffraction at forbidden reflections

2014 J. Phys.: Conf. Ser. 519 012006

(http://iopscience.iop.org/1742-6596/519/1/012006)

Journal of Physics: Conference Series **519** (2014) 012006 doi:10.1088/1742-6596/519/1/012006

Phase transition of KDP observed by Resonant X-ray Diffraction at forbidden reflections

G. Beutier[1,2], S. P. Collins[2], E. N. Ovchinnikova[3], G. Nisbet[2], V. E. Dmitrienko[4]

[1] SIMaP, Grenoble Institute of Technology - CNRS - Grenoble Alpes University, France
[2] Diamond Light Source, Harwell Science & Innovation Campus, OX11 0DE, United Kingdom.
[3] Department of Physics of Moscow State University, 119899 Moscow, Russia
[4] A.V. Shubnikov Institute of Crystallography, 119333, Moscow, Russia

E-mail: guillaume.beutier@simap.grenoble-inp.fr

Abstract. We report observations of space-group-forbidden Bragg reflections in Potassium Dihydrogen Phosphate (KH_2PO_4), also known as KDP, measured by resonant x-ray diffraction at the potassium K edge. We find clear evidence for a transition from one class of space-group-forbidden reflections, where scattering is ruled out by the electric dipole approximation, to a second class, in the ferroelectric phase, where scattering can proceed due to resonant anisotropy within the dipole approximation. The change of symmetry is clearly evidenced by the sudden change of intensity and energy spectrum of the forbidden reflections.

1. Introduction

Diffraction of x-rays, neutrons and electrons is a very sensitive technique for investigations of structural phase transitions because the reduction in symmetry that drives the transition is often heralded by the arrival of weak diffraction peaks that become allowed due to the change in the space group extinction rules. Such a transition from forbidden to allowed scattering can be considered as a special case of a more general hierarchy of scattering processes that involve various ranks of the scattering tensor - in this case, scalar (rank-zero) scattering. When scalar scattering (including Thomson scattering) is forbidden, the crystal symmetry may allow resonant scattering to proceed via anisotropy in the resonant scattering within the electric dipole approximation, described by a second-rank tensor. As symmetry increases, even this process may be annihilated, while allowing higher-rank processes to occur due to some exotic scattering mechanism, described by tensors of rank three or four.

Potassium Dihydrogen Phosphate (KH_2PO_4), also known as KDP is a fascinating test-bed for these processes: the ferroelectric phase transition provides an example of a transition from forbidden- to super-forbidden scattering. Our observations of resonant scattering from KDP, at the potassium K-edge, provide a clear demonstration of this phenomenon.

KDP, and many of its isomorphs, are important hydrogen-bonded ferroelectrics whose properties have long been a source of interest. It spans a wide range of room temperature technological applications, from food additives [1] to optical modulators in non-linear optics [2]. From the physical point of view, it has been mostly studied for its ferroelectricity, being one of the first discovered ferroelectric materials [3]. Indeed, ferroelectricity in KDP arises below

122 K in a complex mechanism that has long been debated. This ferroelectric phase transition has triggered a lot of theoretical advances, based on the pseudospin model initially proposed by Slater [4] and later developed by many authors [5]. It is also an example of soft phonon mode driven phase transition [6]. Experimentally, KDP has been extensively studied against temperature [7], pressure [8], deuteration [9], electric field [10] and mechanical stress [11]. The mechanism is the following: The crystal structure is made of PO_4 tetrahedra linked to each other by hydrogen bonds. The latter consists of individual protons tunnelling between two equivalent quantum wells either side of the mid-point between the tetrahedra. In the paraelectric phase, they tunnel randomly between both sites, whereas in the ferroelectric phase they freeze in a long range ordered pattern. This pattern distorts the structure such that the ionic displacements of the Potassium and Phosphorus ions induces an electric polarisation [12]. The transition is hence at the same time an order-disorder transition for the protons and a displacive transition for the other ions. In the following, we will refer to the ferroelectric phase as the ordered phase and to the paraelectric phase as the disordered phase, since this is the structural detail that matters for the forbidden reflections. After a long controversy, it has been established that the phase transition is of the first order but nearly second order [13].

In this paper we use this now rather well understood phase transition to generalize the concept of forbidden reflections. We will show that the subtle change of symmetry occurring at the phase transition can enable or disable some of the resonant terms involved in forbidden reflections.

2. Theoretical

2.1. Crystal symmetries and forbidden reflections

In the disordered phase, KDP has a tetragonal crystal structure with space group $I\bar{4}2d$, which becomes orthorhombic with space group $Fdd2$ in the ordered phase [14]. The electric polarization of the ordered phase appears along the unique axis of the tetragonal structure. In the following, the settings of the space group $Fdd2$ will be used to describe the crystal. The tetragonal structure will be treated as a special case, since $Fdd2$ is a subgroup of $F\bar{4}d2$, which is another representation of $I\bar{4}2d$. In fact, the description of the disordered phase in the $I\bar{4}2d$ space group corresponds to the average structure, in which the protons have equal probabilities to be in either minima of the double well, but the instantaneous unit cell symmetry does not have such high symmetry. The transformation from the $I\bar{4}2d$ structure to the $F\bar{4}d2$ structure corresponds to a rotation of 45° around the c-axis, which automatically induces a doubling of the unit cell.

In either crystallographic phase, KDP has two types of forbidden reflections: first, the reflections of the type hkl, with h, k, l not all of the same parity, are forbidden by the centring symmetry; secondly, the reflections of the type $h0l$ with $h+l \neq 4n$ and $0kl$ with $k+l \neq 4n$ are forbidden by glide-plane symmetries. The centring symmetry and the glide-plane symmetries survive the phase transition, such that reflections forbidden in one phase remain forbidden in the other phase, preventing an easy observation of the phase transition. This rule is true for scalar atomic scattering factors, but resonant x-rays enhance higher rank tensors which can have non-vanishing structure factors. The reflections forbidden by the centring symmetry are forbidden for all tensors of any rank: their structure factors vanish because of the pure translational symmetry. But in the case of glide-plane forbidden reflections, higher rank tensors can have non-vanishing structure factors. A detailed investigation of the tensor symmetries is necessary to determine which ones participate in the forbidden reflections. We will now focus on reflections that are forbidden by a glide-plane but not by the centring symmetry. They are of the type $h0l$ with h and l even and $h+l=4n+2$, and $0kl$ with k and l even and $k+l=4n+2$. The structure factor F for such reflections of the resonant atomic scattering tensor $\boldsymbol{f}$ is:

$$F(\boldsymbol{f}) = 4\left[\boldsymbol{f} - \hat{S}(\boldsymbol{f})\right] \tag{1}$$

where $\hat{S}$ is the symmetry operator associated with the glide-plane. Therefore, only those tensor components of $\boldsymbol{f}$ which are not invariant with respect to glide-plane symmetry contribute to the diffraction at these reflections. Since these reflections are forbidden, the scalar structure factor vanishes and only resonant atoms, which have enhanced higher rank tensors of scattering, give a significant contribution. In the present case, resonant atoms are the potassium atoms and occupy special positions $8a$ of space group $Fdd2$ (or equivalently at special position $4a$ of space group $I\bar{4}2d$). This crystallographic site has a two-fold axis along 001 (point symmetry ..2) in the orthorhombic phase, which becomes a four-fold rotoinversion axis (point symmetry $\bar{4}$..) in the tetragonal phase. We will see that the change of local symmetry from two-fold axis to four-fold rotoinversion axis is at the origin of drastic changes in the resonant reflections.

2.2. Resonant X-ray Diffraction

Resonant X-ray Diffraction (RXD) is the application to the diffraction geometry of a more general technique now referred as Resonant Elastic X-ray Scattering (REXS). By exciting an electronic transition of the sample, resonant x-rays acquire an enhanced sensitivity to the resonant species and its local environment. It is a powerful probe of electronic orders, including magnetism [15]. REXS is usually described in terms of electronic multipolar resonances. The pure dipole dipole (E1E1) contribution is normally the strongest, but it may cancel out in the structure factor of forbidden reflections, depending on the symmetry of the resonant site, the global symmetry of the crystal, and the considered reflection. Such case allows for easier observation of weaker resonant terms such as mixed dipole-quadrupole (E1E2) terms [16], pure quadrupole-quadrupole (E2E2) terms [17] and maybe higher order electric multipoles when these vanish too. It also allows for easier observation of weaker processes of E1E1 origin such as Thermal Motion Induced (TMI) scattering [18, 19] or Point-Defect Induced (PDI) scattering [18].

Such is the case for resonant forbidden reflections in the disordered phase of KDP at the potassium K edge: because of the $\bar{4}$ axis of the resonant site, the E1E1 tensor is uni-axial and along the 001 axis. It is therefore invariant with respect to the glide-planes of the space group, which all contain the 001 axis, and its structure factor cancels out at the corresponding forbidden reflections. The first non-vanishing tensors are thus third rank tensors. Conversely, the Potassium site in the ordered phase has only a two-fold axis, allowing for additional components of the E1E1 tensor which do not cancel out in the structure factor. The appearance and disappearance, across the phase transition, of the E1E1 term in the structure factor of glide-plane forbidden reflections, has a drastic impact on their intensity and spectrum.

Let us now detail the tensors contributing to the atomic scattering factors and their structure factor at the considered forbidden reflections. We shall use the Cartesian formalism, which is convenient with orthorhombic systems, with axes x, y and z respectively along the 100, 010 and 001 of the orthorhombic structure. Within this framework, the multipolar expansion of REXS up to the electric quadrupole term has the following form [20]:

$$\boldsymbol{f} = \epsilon'^{*}_{\alpha}\epsilon_{\beta}\left[D_{\alpha\beta} + \frac{i}{2}(k_{\gamma}I_{\alpha\beta\gamma} - k'_{\gamma}I^{*}_{\beta\alpha\gamma}) + \frac{1}{4}k'_{\gamma}k_{\delta}Q_{\alpha\gamma\beta\delta}\right] \tag{2}$$

with $\{\alpha,\beta,\gamma,\delta\} \in \{x,y,z\}^4$ and summation over repeated indices is implied. The vectors $\boldsymbol{k}$, $\boldsymbol{k}'$ and $\boldsymbol{\epsilon}$, $\boldsymbol{\epsilon}'$ are the propagation and polarization vectors, respectively, of the incident and scattered radiations. Below we shall also use conventional $\boldsymbol{\sigma}$ and $\boldsymbol{\pi}$ polarization vectors, normal and parallel, respectively, to the scattering plane. Magnetic multipolar and higher order electric multipolar contributions, which are expected extremely weak [21], were omitted. Thus, the resonant scattering tensor consists only of the second rank E1E1 tensor $\boldsymbol{D}$, the third rank E1E2 tensor $\boldsymbol{I}$, and the fourth rank E2E2 tensor $\boldsymbol{Q}$, all of which possessing tensor elements that are sensitive to the incident radiation energy with their own spectrum.

The E1E1 tensor $\boldsymbol{D}$ is of rank 2 and is symmetric in the case of a non-magnetic crystal. Because of the (at least) 2-fold axis at the potassium site, it has the following form [22]:

$$\boldsymbol{D} = \begin{pmatrix} D_{xx} & D_{xy} & 0 \\ D_{xy} & D_{yy} & 0 \\ 0 & 0 & D_{zz} \end{pmatrix} \tag{3}$$

Following equation 1, its structure factor at the glide-plane forbidden reflections is:

$$F(\boldsymbol{D}) = 4\left[\boldsymbol{D} - \hat{S}(\boldsymbol{D})\right] = 8\begin{pmatrix} 0 & D_{xy} & 0 \\ D_{xy} & 0 & 0 \\ 0 & 0 & 0 \end{pmatrix} \tag{4}$$

If D_{xy} is not zero for any symmetry reason and if the E1E1 term is considerably stronger than any other term, as it is usually the case, the spectrum of the forbidden reflection is unique, independently of the chosen forbidden reflection, its azimuth, and the beam polarization (after correction for self-absorption effects, taking into account linear dichroism [23]). We will show that it is the case in the ordered phase. In the disordered phase, the 2-fold axis becomes a pseudo 4-fold axis, and the off-diagonal terms of symmetric rank 2 tensors vanish [22]: $D_{xy} = 0$, thus cancelling out the structure factor: above the transition the reflection is forbidden for scattering tensors up to the rank 2, whereas below the transition it is forbidden only for rank 0 (scalars). This can be seen as an extension of the concept of forbidden reflections, usually understood as for scalar scattering factors.

In absence of E1E1 scattering, it is necessary to extend the analysis to weaker scattering processes represented by higher order tensors. E1E2 (third-rank tensor) and E2E2 (fourth-rank tensor) resonances are usually the strongest ones, along with the TMI term (third-rank tensor). PDI scattering is also expected to have a sizeable effect in the paraelectric phase of KDP, because of the static disorder of the protons [24]. Here we detail the analysis for the E1E2 term only, only to show that it does not vanish. The symmetry properties of third rank tensors representing TMI and PDI scattering differ slightly from that of the E1E2 term [25].

Any third rank Cartesian tensor $\boldsymbol{T}$ with $\bar{4}$ symmetry has six independent components [22, 26]: $T_{xxz} = -T_{yyz}$, $T_{zxx} = -T_{zyy}$, $T_{xzx} = -T_{yzy}$, $T_{xyz} = T_{yxz}$, $T_{xzy} = T_{yzx}$ and $T_{zxy} = T_{zyx}$. In the notation scheme of [22]:

$$\boldsymbol{T} = \left(\begin{array}{ccc|ccc|ccc} 0 & 0 & 0 & T_{xyz} & T_{xzx} & 0 & T_{xzy} & T_{xxz} & 0 \\ 0 & 0 & 0 & -T_{xxz} & T_{xzy} & 0 & -T_{xzx} & T_{xyz} & 0 \\ T_{zxx} & -T_{zxx} & 0 & 0 & 0 & T_{zxy} & 0 & 0 & T_{zxy} \end{array}\right) \tag{5}$$

By applying the glide-plane symmetry, the general structure factor for a third rank tensor is left with 3 independent components [27]:

$$F(\boldsymbol{T}) = 4\left[\boldsymbol{T} - \hat{S}(\boldsymbol{T})\right] = 8\left(\begin{array}{ccc|ccc|ccc} 0 & 0 & 0 & T_{xyz} & 0 & 0 & T_{xzy} & 0 & 0 \\ 0 & 0 & 0 & 0 & T_{xzy} & 0 & 0 & T_{xyz} & 0 \\ 0 & 0 & 0 & 0 & 0 & T_{zxy} & 0 & 0 & T_{zxy} \end{array}\right) \tag{6}$$

Additionally, the E1E2 tensor $\boldsymbol{I}$ has the following property by construction [20]: $I_{\alpha\beta\gamma} = I_{\alpha\gamma\beta}$ for all $\{\alpha, \beta, \gamma\} \in \{x, y, z\}^3$. Its structure factor at the glide-plane forbidden reflections is left with two independent components, I_{xyz} and I_{zxy}:

$$F(\boldsymbol{I}) = 8\left(\begin{array}{ccc|ccc|ccc} 0 & 0 & 0 & I_{xyz} & 0 & 0 & I_{xyz} & 0 & 0 \\ 0 & 0 & 0 & 0 & I_{xyz} & 0 & 0 & I_{xyz} & 0 \\ 0 & 0 & 0 & 0 & 0 & I_{zxy} & 0 & 0 & I_{zxy} \end{array}\right) \tag{7}$$

Note that equation 7 is valid only in the disordered phase, as additional components of the tensor appear in the ordered phase with the reduction of symmetry. We see that third-rank tensors do not vanish in general in the disordered phase. In addition to the E1E2 term, one can show that the third-rank tensor representing TMI and PSI scattering also contributes to forbidden reflections. A similar analysis of the fourth-rank tensor representing E2E2 processes reveals that a single independent component survives in the structure factor. With several independent components of presumably similar amplitudes contributing to the tensor structure factor in the disordered phase, one can expect a dependence of the spectrum with the chosen reflection, its azimuth, and the polarisation.

In conclusion, REXS at forbidden reflections is dominated by the E1E1 tensor in the ordered phase, but it vanishes in the disordered phase, unveiling contributions from weaker resonant processes. We expect therefore a large difference of intensity between the two phases, in favour of the ordered phase. Since different tensors are involved, we also expect a change in the energy spectrum of the forbidden reflections.

3. Experimental

A single crystal of KDP with surface normal 001 was measured at beamlines I16 of Diamond Light Source [28] and BM28 (XMaS) of the European Synchrotron Radiation Facility. The sample was enclosed in a closed-cycle cryofurnace and the temperature varied between 60 K and 400 K (I16) or 15 K and 320 K (XMaS). The lattice parameters of the orthorhombic phase are a=10.53 Å, b=10.44 Å, c=6.90 Å[29]. The 002 and 402 forbidden reflections were measured at the potassium K edge (∼3.608 keV). Below the phase transition, the sample forms two types of domains related by a 90° rotation around the 001 axis. The a and b lattice parameters are not different enough to separate the 402 reflection of one domain type from the 042 reflection of the other domain type without using an analyser: the results presented below on the 402 reflection should be understood as a mixture of 402 and 042. The natural linear polarization of the beam was used. Most measurements were done without polarization analysis, with limited polarization analysis using the 111 reflection of a gold single crystal. The azimuthal reference is the (110) axis (equivalent to a (100) axis in the tetragonal basis) and the azimuth is zero when the azimuthal reference is in scattering plane. We found that KDP suffered from radiation damage from the full direct beam of I16 with its usual focus (120 μm x 30 μm, HxV). The beam was therefore unfocused and sufficiently attenuated to yield reproducible measurements during successive scans. A shift of 3 eV was found between the energy calibrations of both beamlines and we have rescaled the data presented here to the calibration of I16, which yields data more consistent with absorption spectra at the potassium K edge found in the literature [30, 31].

Figure 1 shows the temperature dependence of the 202 allowed reflection and the 002 forbidden reflection. The ferroelectric phase transition can be seen on both reflections around 120 K. The allowed reflection shows a strong broadening due to the formation of domains at low temperature. The forbidden reflection shows a huge change of intensity across the phase transition, due to the appearance (during warming) or disappearance (during cooling) of the E1E1 contribution, as explained above. The first order character of the transition is clearly seen on the integrated intensity of the 002 reflection, with a difference of critical temperature of about 2 K between warming and cooling (insert of Figure 1 bottom left). For each cycle, the integrated intensity can be reasonably fitted with a power law: $I = I_0 \left(1 - \frac{T}{T_c}\right)^{2\beta} + C$ (C accounting for the third rank tensors contribution, supposed temperature independent on this range), with a critical exponent $\beta \approx 0.23$. The reasonable agreement with a power law shows why this phase transition has been considered for long as second order and is now said almost second order.

Above the transition, the system displays a regular evolution. The 202 reflection sharpens but its integrated intensity remains constant. The 002 reflection also sharpens (Figure 1, bottom

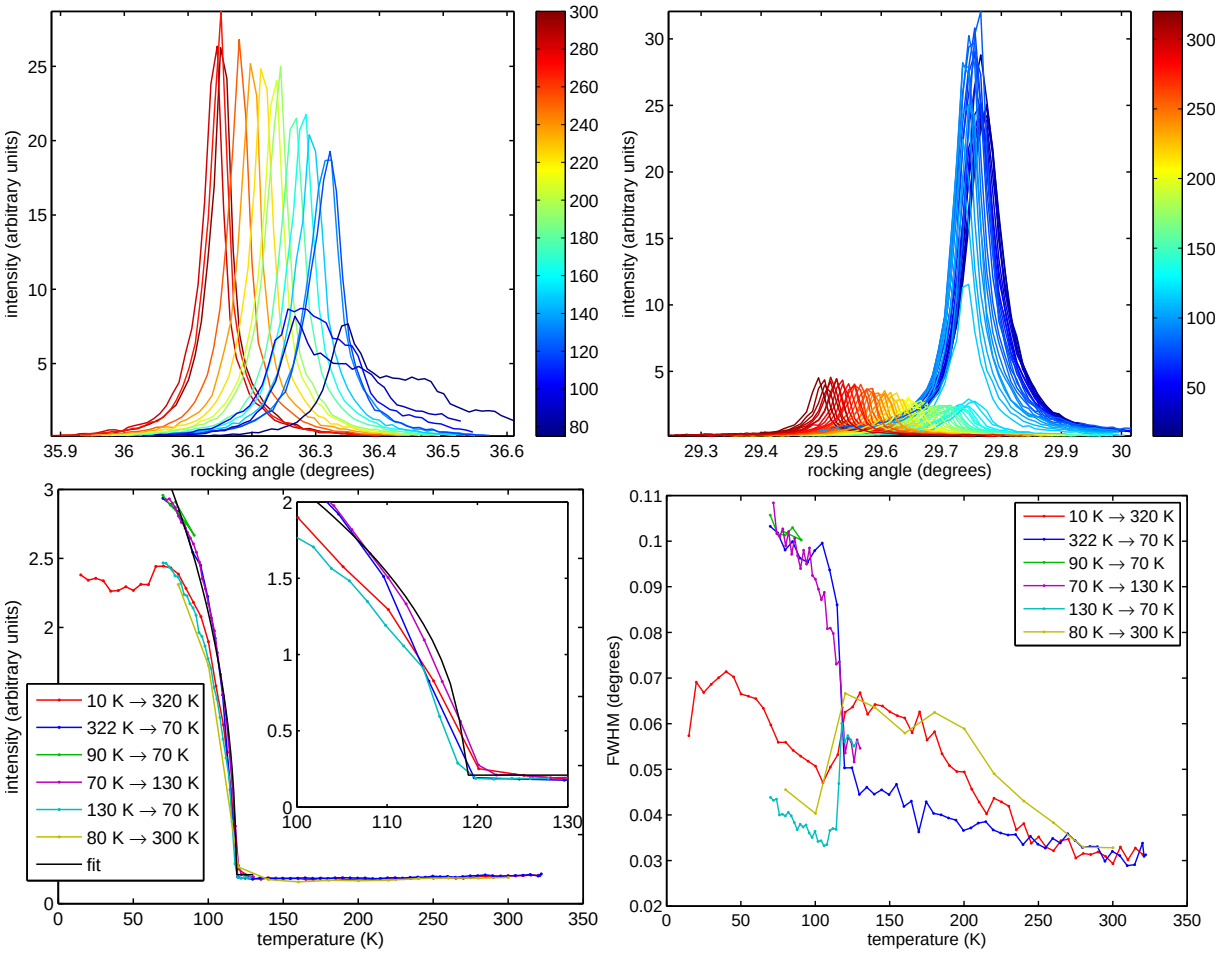

Figure 1. Temperature dependence of the 202 allowed reflection (top left) and 002 forbidden reflection (top right). The 002 reflection was measured at 3.6095 keV and azimuth -84°. Bottom: integrated intensity (left) and full-width at half-maximum (right) of the 002 reflection during several temperature cycles. A fit of the integrated intensity of the fourth temperature dependence is shown (see text for details).

right), and its integrated intensity increases smoothly with the temperature. This increase can be ascribed to TMI scattering, which grows with the activation of harmonic vibrations [18]. A reasonable fit of this increase can be obtained with the phenomenological model proposed in [32]. However PDI scattering, due to the increase of defects in the hydrogen configuration, is likely to contribute too, with a different temperature dependence. Further analysis is in progress and will be reported elsewhere [24].

The ferroelectric transition is unambiguously evidenced, not only on the rocking curve intensity at fixed energy, but also on the whole spectrum as a function of temperature (Figure 2). While there is little change of lineshape for the 002 reflection from room temperature to 122 K, the phase transition induces a strong change due to the enabling of the E1E1 channel, and remains again stable in the low temperature range (Figure 2, top row). This sudden change of intensity and lineshape was also observed on the 402 (Figure 2, middle row). In the temperature range above the phase transition, both reflections show a temperature dependence of the spectrum, which can be related to TMI and PDI scattering [24]. The effect is larger on the 402 than on the 002, largely because these effects are proportional to the square modulus of the scattering

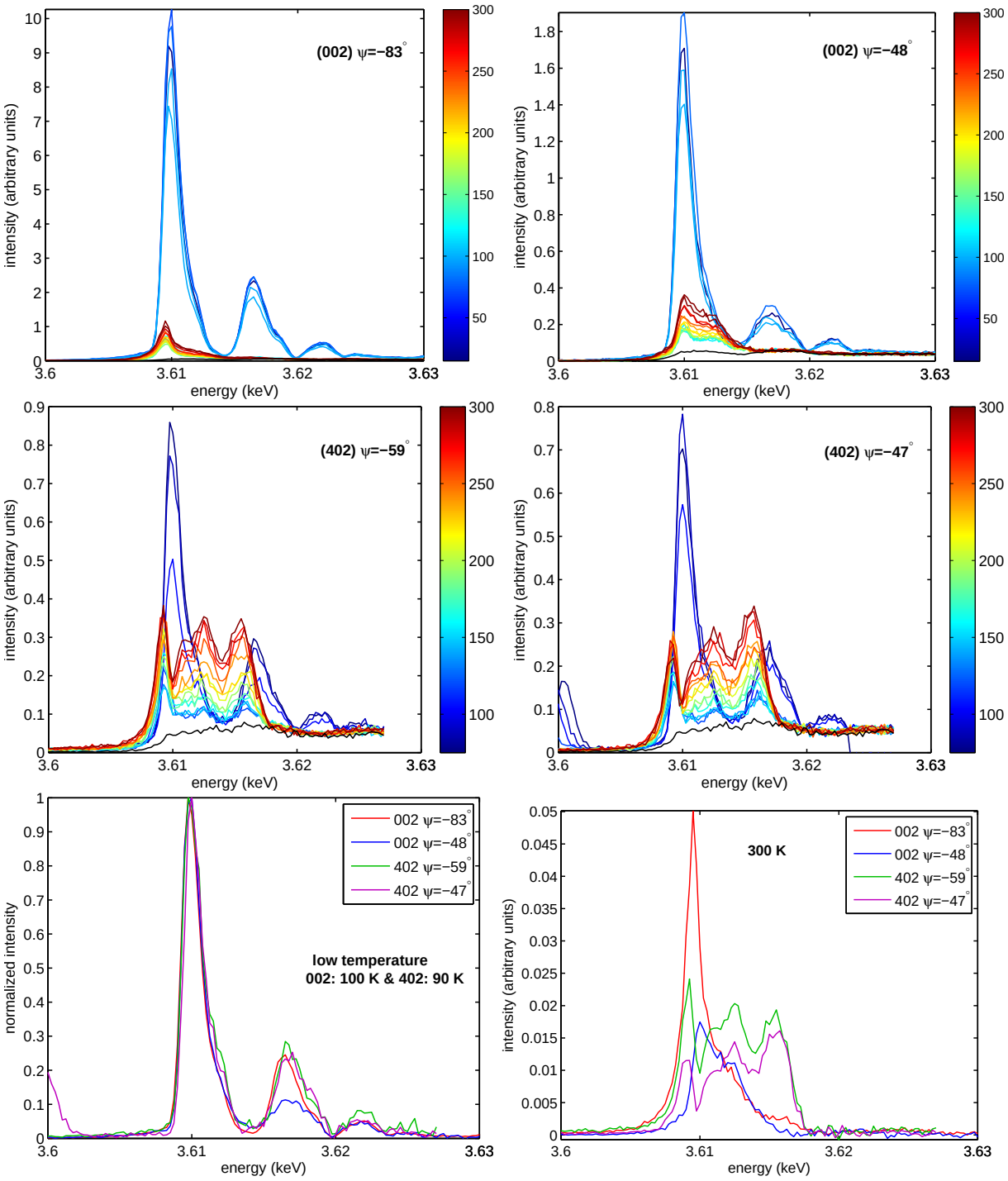

Figure 2. Temperature dependence of the forbidden reflection spectra: 002 (top row) at azimuth -83° (left) and -48° (right), and 402 (middle row) at azimuth -59° (left) and -47° (right). Intensities were normalized by the incident beam intensity but no further correction was applied. The black curves in these panels show the fluorescence background. Colour bars show the temperature scale. Bottom row: comparison of the 002 and 402 reflection spectra at two different azimuths ψ each, at low temperature (left) and room temperature (right). The low temperature data have been normalized by the peak value of each spectrum. The strong intensity below 3.605 keV on one of the low temperature curves is ascribed to multiple scattering.

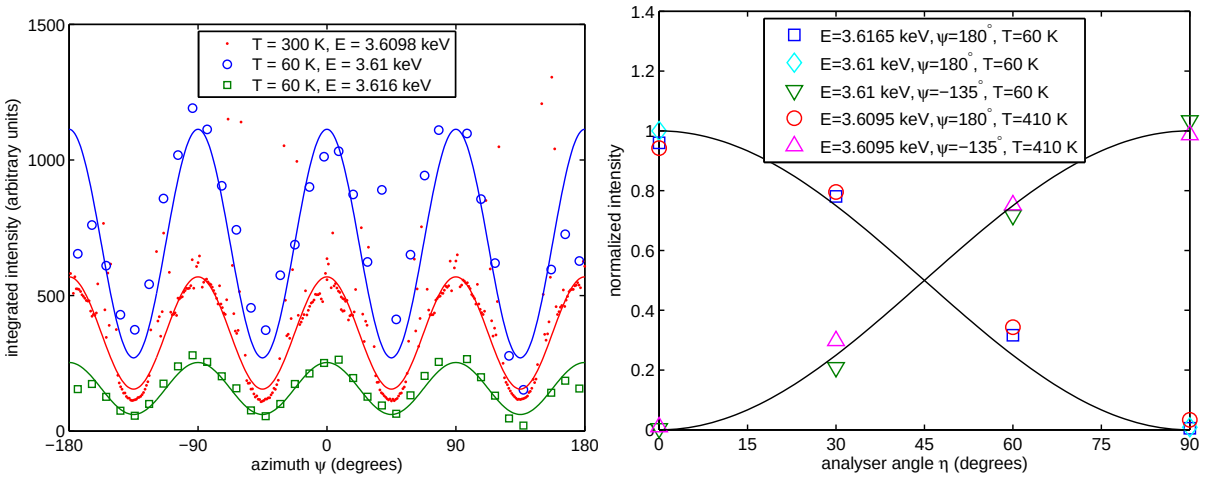

Figure 3. Azimuthal dependence without polarisation analysis (left) and polarisation analysis (right) of the 002 forbidden reflection. Intensities were integrated over rocking curves. Continuous lines are fits against the models described in the text. The continuous black lines in the right panel show $\sin^2\eta$ and $\cos^2\eta$.

vector [23]. The azimuth also plays a role. As predicted above, the low temperature spectrum is identical in shape for the 002 and 402 forbidden reflections and independent of the azimuth (Figure 2, bottom left). This demonstrates that a single tensor component (D_{xy}) dominates the intensity. There is nevertheless a small deviation for one of the curves around 3.615 keV, which we cannot explain without invoking interference with competing multiple scattering. Above the transition, the spectrum depends on the chosen reflection and on the azimuth (Figure 2, bottom right), due to the participation of several tensor components.

Let us now examine the azimuthal dependence and polarization properties of the 002 forbidden reflections (Figure 3): both phases ($T < 122$ K and $T > 122$ K) have the same polarisation properties and similar azimuthal dependence. In the following we consider only the E1E1 and E1E2 processes: the E2E2 contribution are expected to be weak compared to that of E1E2, according to calculations performed with the code FDMNES [33]. By projecting the polarisation vectors and wave vectors onto the E1E1 and E1E2 tensors given in equations 4 and 6, we obtain the structure factors for the polarisation channels $\sigma \to \sigma$ and $\sigma \to \pi$:

$$F^{\sigma\sigma}_{E1E1}(002) = -D_{xy}\cos 2\psi \tag{8}$$
$$F^{\sigma\pi}_{E1E1}(002) = D_{xy}\sin\theta\sin 2\psi \tag{9}$$
$$F^{\sigma\sigma}_{E1E2}(002) = 2I_{xyz}\sin\theta\cos 2\psi \tag{10}$$
$$F^{\sigma\pi}_{E1E2}(002) = \left[I_{zxy}\cos^2\theta + I_{xyz}\left(2-3\cos^2\theta\right)\right]\sin 2\psi \tag{11}$$

where θ is the Bragg angle and ψ the azimuthal angle, such that $\psi = 0$ when the 110 direction (which is the 100 direction in the tetragonal basis) lies in the scattering plane pointing away from the incident beam. For both E1E1 and E1E2, and therefore in both phases, the $\sigma \to \sigma$ channel vanishes at $\psi = 45°\,[90°]$ and the $\sigma \to \pi$ channel vanishes at $\psi = 0\,[90°]$, as shown in the right panel of Figure 3.

In the ordered phase, we consider only the E1E1 term and neglect higher rank processes. The scattered intensity with σ-polarized incident beam and no polarization analysis is:

$$I^{\sigma}(002) \approx |F^{\sigma\sigma}_{E1E1}(002)|^2 + |F^{\sigma\pi}_{E1E1}(002)|^2 = |D_{xy}|^2\left(1-\cos^2\theta\sin^2 2\psi\right) \tag{12}$$

The data at 60 K of Figure 3 were fitted with this equation, with $|D_{xy}|^2$ as unique free parameter. In the disordered phase, $D_{xy} = 0$ and we consider only the E1E2 contribution:

$$I^{\sigma}(002) \approx |F^{\sigma\sigma}_{E1E2}(002)|^2 + |F^{\sigma\pi}_{E1E2}(002)|^2 = I^{\sigma}_0 \left(1 - a \sin^2 2\psi\right) \quad (13)$$

where I^{σ}_0 and a are functions of I_{xyz}, I_{zxy} and θ, and thus depend strongly on the energy. The data at 300 K of Figure 3 were fitted with this equation, with I_0 and a as free parameters. In both phases the azimuthal dependence of the 002 reflection is four-fold and even, with maxima and minima at $\psi = 0[\pi/2]$ and $\psi = \pi/4[\pi/2]$, in agreement with experimental data. The change of symmetry of the potassium site is not visible on the azimuthal scans of the 002 reflection, which is expected since both -4 and ..2 symmetries give four-fold symmetry of the intensity along the symmetry axis. However, the contrast of the four-fold oscillation should vary strongly with the energy in the disordered phase (equation 13), while it is constant in the ordered phase (equation 12). This constant ratio allows reasonable fitting of the low temperature data, but there is unfortunately only one set of data in the disordered phase, not enough to demonstrate the change of ratio with the energy.

4. Conclusion

Forbidden reflections can be seen as a more general concept than just the cancellation of the scalar structure factor. The concept can be extended to higher rank tensors, which are relevant in REXS. In particular, while it is common to witness an order-disorder phase transition by the (dis)appearance of a non-resonant (rank 0) forbidden reflection, we have seen in this report that we can monitor the order-disorder phase transition of KDP by measuring the second rank tensor of REXS, which becomes forbidden in the disordered phase. Beyond the fundamental interest in the diffraction process for itself, this method can be useful for crystals like KDP in which the phase transition do not change the extinction conditions of non-resonant reflections. In the case of a less known structure, the disappearance of the second rank tensor during a phase transition yield a valuable information on the site symmetry.

References

[1] http://en.wikipedia.org/wiki/Monopotassium_phosphate
[2] Franken P A and Ward J F 1963 *Rev. Mod. Phys.* **35** 23–39
[3] Busch G 1938 *Helv. Phys. Acta* **11** 269
[4] Slater J C 1941 *J. Chem. Phys.* **9** 16
[5] Blinc R and Zeks B 1972 *Advances in Physics* **21** 693–757
[6] Scott J F 1974 *Rev. Mod. Phys.* **46** 83–128
[7] Nelmes R J, Meyer G M and Tibballs J E 1982 *J. Phys. C : Solid State Phys.* **15** 59–75
[8] Tibballs J E, Nelmes R J and McIntyre G J 1982 *J. Phys. C : Solid State Phys.* **15** 37–58
[9] Loiacono G, Balascio J and Osbourne W 1974 *Appl. Phys. Lett.* **24** 455
[10] van Reeuwijk S J, Puig-Molina A and Graafsma H 2001 *Phys. Rev. B* **64** 134105
[11] Lisnii B M, Levitskii R R and Baran O R 2007 *Phase Transitions* **80** 25–30
[12] Cochran W 1961 *Advances in Physics* **10** 401–420
[13] Reese W 1969 *Phys. Rev.* **181** 905
[14] Frazer B and Pepinsky R 1952 *Phys. Rev.* **85** 479–480
[15] Beale T, Beutier G, Bland S, Bombardi A, Bouchenoire L, Buñau O, Matteo S D, Fernández-Rodríguez J, Hamann-Borrero J, Herrero-Martín J, Jacques V, Johnson R, Juhin A, Matsumura T, Mazzoli C, Mulders A, Nakao H, Okamoto J, Partzsch S, Princep A, Scagnoli V, Strempfer J, Vecchini C, Wakabayashi Y, Walker H, Wermeille D, and Yamasaki Y 2012 *Eur. Phys. J. Special Topics* **208** 89–98
[16] Templeton D H and Templeton L K 1994 *Phys. Rev. B* **49** 14850
[17] Dmitrienko V E, Ovchinnikova E N, Collins S P, Nisbet G and Beutier G 2014 *Journal of Physics: Conference Series* **this volume**
[18] Dmitrienko V E and Ovchinnikova E N 2000 *Acta Cryst. A* **56** 340–347
[19] Kokubun J, Kanazava M, Ishida K and Dmitrienko V 2001 *Phys. Rev. B* **64** 073203

[20] Blume M 1994 *Magnetic Effects in Anomalous Dispersion // in Resonant Anomalous X-ray Scattering, Edited by Materlik G., Sparks C.J., Fisher K. Amsterdam* (Elsevier)
[21] Joly Y, Collins S P, Grenier S, Tolentino H C N and Santis M D 2012 *Phys. Rev. B* **86** 220101(R)
[22] Authier A 2003 *International Tables for Crystallography.* vol D
[23] Beutier G, Collins S, Nisbet G, Ovchinnikova E and Dmitrienko V 2012 *Eur. Phys. J. Special Topics* **208** 53–66
[24] in preparation
[25] Mukhamedzhanov E K, Kovalchuk M V, Borisov M M, Ovchinnikova E N, Troshkov E V and Dmitrienko V E 2010 *Crystallography Reports* **55** 174–181
[26] We spotted an error in reference [22], 1.1.4.8.5.5.: the term 333 should be absent, which is consistent with six independent components, as claimed in the reference.
[27] In the tetragonal basis with axes turned by 45°, the non-vanishing components would be the other ones: I_{xxz}, I_{xzx} and I_{zxx}.
[28] Collins S, Bombardi A, Marshall A, Williams J, Barlow G, Day A, Pearson M, Woolliscroft R, Walton R, Beutier G and Nisbet G 2010 *AIP Conf. Proc.* **1234** 303–306
[29] Levy H A, Peterson S W and Simonsen S H 1954 *Phys. Rev.* **93** 1120–1121
[30] Williams G P 2009 *X-ray data booklet* (Lawrence Berkeley National Laboratory) chap Electron binding energies
[31] Cibin G, Mottana A, Marcelli A and Brigat M F 2005 *Mineralogy and Petrology* **85** 67–87
[32] Collins S, Laundy D, Dmitrienko V, Mannix D and Thompson P 2003 *Phys. Rev. B* **68** 064110
[33] Joly Y 2001 *Phys. Rev. B* **63** 125120